Radiative emission dynamics of quantum dots in a single cavity micropillar

M. Schwab, H. Kurtze, T. Auer, T. Berstermann, and M. Bayer
Experimentelle Physik II, Universität Dortmund, D-44221 Dortmund, Germany

J. Wiersig, N. Baer, C. Gies, and F. Jahnke
Institute for Theoretical Physics, University of Bremen, D-28334 Bremen, Germany

J. P. Reithmaier and A. Forchel
Technische Physik, University of Würzburg, Am Hubland, D-97074 Würzburg, Germany

M. Benyoucef and P. Michler
5th Physics Institute, University of Stuttgart, D-70550 Stuttgart, Germany

(Received 10 October 2005; revised manuscript received 18 June 2006; published 25 July 2006)

The light emission of self-assembled (In,Ga)As/GaAs quantum dots embedded in single GaAs-based micropillars has been studied by time-resolved photoluminescence spectroscopy. The altered spontaneous emission is found to be accompanied by a nonexponential decay of the photoluminescence where the decay rate strongly depends on the excitation intensity. A microscopic theory of the quantum dot photon emission is used to explain both the nonexponential decay *and* its intensity dependence. Also the transition from spontaneous to stimulated emission is studied.

DOI: 10.1103/PhysRevB.74.045323 PACS number(s): 73.21.La, 71.36.+c, 78.47.+p, 42.65.−k

I. INTRODUCTION

The possibility of altered spontaneous emission by modifying the photonic environment, known as the Purcell effect,[1] allows one to tailor the optical emission properties of quantum dots (QDs). Spontaneous emission is caused by fluctuations of the vacuum electromagnetic field, so that its change represents a true quantum effect. The photonic environment can be altered by modifying the density of optical modes, to which the QD electronic transitions can couple, and/or by modifying the amplitude of the vacuum field at the QD location. Both changes have been achieved by placing the QDs in a resonator structure with size of the order of the light wavelength, in which the electromagnetic field is three-dimensionally confined.[2–7] As a consequence the mode spectrum becomes discretized, and the vacuum field amplitude can be significantly modified.

The light emission of QDs in optical cavities has been a very active field of solid state research during recent years. The altered spontaneous emission dynamics of QDs has been demonstrated using different resonator types, such as microdisk structures,[2] patterned cavity pillars,[3–6] or photonic crystal defects.[7] Its experimental verification requires time-resolved photoluminescence (PL) measurements. Since QDs are often considered as artificial atoms, it became a standard in these studies to use the exponential decay known from two-level emitters and to carry it over to a QD system in order to quantify the emission dynamics and in particular the Purcell effect. Then the decay time τ of the emitter in the presence of the cavity follows from

$$\frac{\tau_0}{\tau} = \frac{2}{3} F_P \frac{|\vec{E}(\vec{r})|^2}{|\vec{E}_{max}|^2} \frac{\Delta\lambda_c^2}{4(\lambda_e - \lambda_c)^2 + \Delta\lambda_c^2} \cos^2\vartheta + \frac{\tau_0}{\tau_{leak}}, \quad (1)$$

where τ_0 is the decay time in a spatially homogeneous medium, which is determined by the Weisskopf-Wigner decay rate.[8] The second term on the right-hand side models the emission into leaky modes. The first term describes the QD emission at wavelength λ_e into a cavity mode at wavelength λ_c. An emitter at location $\vec{r}$ is subject to an electric field $\vec{E}(\vec{r})$ whose amplitude varies between the maximum value $|\vec{E}_{max}|$ in a field antinode and zero for a node position. ϑ is the angle between the electric-field vector and the dipole moment of the electronic transition.

The Purcell factor F_P gives the enhancement of the emission decay rate in the resonator in comparison to the homogeneous medium,

$$F_P = \frac{3\lambda_e^3}{4\pi^2 n^3} \frac{gQ}{V_c}. \quad (2)$$

Here, Q is the quality factor, V_c is the effective mode volume in the cavity with refractive index n, and g is the mode degeneracy. The application of Eq. (1) requires that the emitter linewidth $\Delta\lambda_e$ is much smaller than the cavity linewidth $\Delta\lambda_c$. This is well fulfilled for QDs at cryogenic temperatures.

A closer inspection of the literature reveals, however, that in many cases a nonexponential decay of the time-resolved PL is observed for a wide variety of QD resonator systems,[9–11] and even for QDs without optical cavities.[12,13] While this in itself complicates the quantification of the altered spontaneous emission in terms of a constant decay time, we additionally report a strong dependence of the time-resolved PL decay on the excitation intensity, also far below the stimulated emission regime. The decay rate continuously increases from the weakest possible pumping, for which we can detect a PL signal, up to the laser threshold. Our experimental results are obtained by time-resolved PL measurements using (In,Ga)As/GaAs QDs in GaAs-based pillar microcavities. In these resonators, two distributed Bragg reflector (DBR) mirrors provide the optical confinement

along the vertical direction. The patterning in the form of pillars provides an additional efficient mode confinement in transverse direction due to total internal reflection. Using micro-PL, the emission of individual pillars can be analyzed after excitation of the QDs with a short laser pulse.

In the past, various effects have been proposed to explain the frequently observed nonexponential decay of the PL under these conditions: For example, the experimental data were recorded from a QD ensemble. As the emitter locations vary inside the resonator, for each position a different decay rate is expected from Eq. (1). Hence the integrated intensity measured in the experiment does in general not exhibit a monoexponential decay. In addition, the ensemble exhibits fluctuations in the QD emission energies and dipole matrix elements, which might lead to deviations from a single exponential decay. In our calculations, these effects were included. For the studied situation, they influence only weakly the shape of the time-resolved PL signal. Additional experimental evidence that the different positions in the cavity and variations of the QD emission energies are not the prime reason for the nonexponential character of the decay can be obtained from studies of the time-resolved PL signal for QDs without microcavity, which is otherwise not the subject of this paper.[14] While the microcavity enhances the nonexponential shape of the decay, also without microcavity the effect can be observed.

As a further alternative, coupling of bright and dark exciton states via spin-flip processes has been suggested as an origin for the nonexponentiality.[15,16] We discuss in detail below that this mechanism can be ruled out for the present experiments as well. Furthermore, none of the alternative mechanisms can explain the observed strong dependence on the excitation intensity.

Based on a microscopic theory for QD carriers interacting with the quantized light field, we analyze the time-resolved PL. The underlying set of equations is referred to as semiconductor luminescence equations (SLE), which have been used in the past for quantum well systems.[17] While the PL of an (ideal) ensemble of two-level emitters shows an exponential decay with a time constant independent of the excitation conditions, this is found to be very different for semiconductor QDs. The recombination of an excited electron requires the presence of a hole. Scattering and dephasing processes reduce the correlation between optically generated electron-hole pairs and thus lead to a distinct departure from the simple two-level picture (corresponding to independent excitons with fully correlated electron-hole states). Our calculations of the electron-hole recombination reveal the intrinsic nature of the nonexponential decay and its excitation intensity dependence. While other (extrinsic) processes could be important in other specific experiments, they do not show the discussed intensity dependence and are limited to special systems or excitation conditions.

The paper is organized as follows. In the next section we discuss the samples under study as well as the experimental technique. In Sec. III we present the experimental results and give a preliminary analysis. In Sec. IV the theoretical model is introduced and the relation to the experiment is discussed in detail. The paper is concluded by a summary.

II. SAMPLE AND EXPERIMENT

The planar microcavity sample was grown by molecular beam epitaxy on a (100)-oriented undoped GaAs substrate, with a GaAs buffer layer of 0.4 μm thickness. The GaAs λ-cavity layer was sandwiched between two DBRs, consisting of 23 and 20 alternating AlAs/GaAs films for the bottom and the top mirrors, respectively. Each film is made from a 79-nm-thick AlAs and a 67-nm-thick GaAs $\lambda/4$ layer. A single layer of self-assembled (In,Ga)As/GaAs QDs serves as optically active medium in the center of the resonator, where the vertical electric-field amplitude has an antinode, to maximize the light-matter interaction in the planar cavity case. The nominal material composition of the QDs is InAs, but during growth intermixing with the GaAs barriers occurs. As the precise, position-dependent material composition is not available, we use the generic term (In,Ga)As for the QD material. The QD surface density is $\approx 3\times 10^{10}$ cm^{-2}. Single pillar microcavities with different diameters ranging from about 1 to 6 μm and spaced 400 μm apart were fabricated by electron-beam lithography and dry etching.[18] Due to this patterning the field strength is modulated in the cavity plane.

The pillar microcavities were mounted on the cold finger of a microscopy flow cryostat allowing for temperature variations down to 6 K. In time-integrated photoluminescence spectroscopy, a frequency doubled Nd:YAG laser was used for continuous wave optical excitation at $\lambda = 532$ nm. For time-resolved photoluminescence, a pulsed Ti:sapphire laser with pulse durations of ≈ 100 fs was used. The laser beams were focused onto the sample by a microscope objective with a focal length of 1.3 cm, by which a spot diameter of about 10 μm could be reached. This diameter is larger than that of the largest studied cavity, so that one can assume homogeneous excitation conditions.

We note that the laser excitation does not lead to any sizeable sample heating effects in the microscopy cryostat. This has been checked by performing time-resolved experiments with the sample inserted in superfluid helium ($T = 2$ K) in an optical bath cryostat. Under otherwise identical excitation conditions, the same behavior is observed for the micropillar photoluminescence kinetics as the one described in Sec. III.

In particular, the measured time evolution of the PL depends strongly on the excitation power. In the following we give the average power density P_{exc}, which is connected to the energy per laser pulse J_{pulse}, focused into a spot with area A, by $P_{exc}\times A = f \times J_{pulse}$, where $f = 75.6$ MHz is the pulse repetition rate. A laser power of 1 mW (corresponding to a power density of 1.27 kW cm^{-2}, which is a typical value for high excitation in the experiment) is achieved for a pulse energy of ~ 0.013 nJ. With an excitation energy of 1.55 eV (wavelength ~ 800 nm as in experiment) per electron-hole pair, about 5.2×10^8 of such pairs could be created. Further we assume that within the λ-cavity only about 0.01% of the incident laser power is converted into carriers, which may be trapped in the wetting layer and relax further towards the QD ground state. This is estimated from comparing the relative emission intensities of the QDs with that of bulk GaAs. Distributing 0.01% of the carriers over the excitation area leads to an estimate of $n_{eh} \approx 6.8\times 10^9$ cm^{-2} for the carrier density.

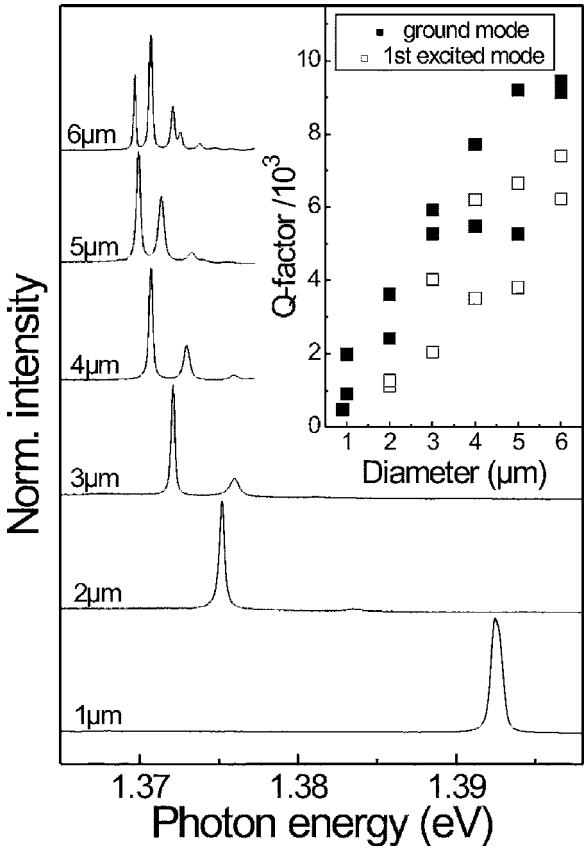

FIG. 1. PL emission spectra from single cylindrically shaped micropillar structures of varying diameters. The inset gives the quality factors of the two energetically lowest photon modes as function of the pillar diameter. Solid (open) symbols give data for the fundamental (first excited) mode. $T=6$ K.

Carrier densities in this range have also been used in the numerical analysis, see Sec. IV.

Some effects have not been considered in this simple estimate, because they are difficult to quantify. For example, the true carrier density may be reduced due to above-stop-band reflection. On the other hand, an increase might occur due to reabsorption of light emitted from GaAs, such as from the substrate. Our cavities operate in the weak-coupling regime, so that effects known from strong coupling play no role here. Note that the variations in the carrier density due to these additional effects are expected to be small.

Excitation and collection were done through the microscope. After light collection, the emission was directed into a 0.5-m monochromator where the signal could be sent either to a charge-coupled device camera for time-integrated PL studies (used also for alignment) or to a streak camera for time-resolved experiments with a resolution of $\approx$20 ps.

In Fig. 1 the emission spectra of single pillars with different diameters are shown, obtained by excitation with the Nd:YAG laser. For better comparison, the intensity has been normalized. With decreasing size the energies of the optical modes shift to higher frequencies. In addition the splitting between the modes increases strongly. These observations are in accordance with previous studies of the optical mode spectrum in similar patterned cavities.[19–25] We note that the inhomogeneously broadened QD emission spectrum has a full width at half maximum of about 30 meV at low excitation. The emission is centered around 1.38 eV, so that the QD ensemble represents a light source which provides emission over the energy range in which the fundamental modes of the studied optical resonators are located.

We have studied the PL decay of the QDs across their inhomogeneously broadened emission band (by analyzing the emission along the plane of an unpatterned resonator and by studying a QD reference sample). An initial decay time of 600 ± 50 ps is observed at 0.17 kW cm^{-2} with no correlation to the emission energy. Therefore any cavity size dependence of the carrier lifetime cannot be related to systematic variations of the dipole coupling with emission energy due to changes of the QD confinement.

The inset of Fig. 1 gives the pillar diameter dependence of the quality factors $Q=E/\Delta E$ of the optical modes. Data for the two lowest confined modes are shown: in both cases we find a considerable decrease in Q with decreasing pillar size. While for the 6-μm-diameter pillars the quality factors are almost 10 000, the cavity quality for the smallest cavities with 1 μm diameter varies depending on the resonator from 2000 to below 1000. Also for larger cavity diameters, sample-dependent variations of the cavity quality are observed. Furthermore, the first excited mode has always a smaller Q than the fundamental mode. However, one has to be careful in such a comparison, as an increased linewidth of the corresponding emission might arise from a slight mode splitting, which has been predicted in Ref. 26 for the first excited mode. Within our experimental accuracy (0.2 meV resolution of the setup), this mode splitting lies below the mode linewidth due to the finite photon lifetime. Independent of the involved photon mode, the decrease of Q with decreasing pillar size arises from reduced confinement of the mode for small cavities and also from an increased importance of surface roughness scattering at the sidewalls.

III. EXPERIMENTAL RESULTS

Figure 2 shows the decay of the time-resolved PL for detection at the energy of the respective fundamental optical mode of micropillars with different diameters. The intensity is plotted on a logarithmic scale. Excitation was done with the pulsed Ti:sapphire laser, with the wavelength set to 800 nm, corresponding to creation of carriers in the GaAs barriers, to allow for a variation of excitation power and therefore carrier density over wide ranges. This wavelength is also above the stop band of the planar resonator. The used low excitation power of 1.3 kW cm^{-2} guarantees that the observed PL occurs in the spontaneous emission regime.

The faster decay for decreasing pillar diameter is mainly a consequence of the confinement induced enhancement of the vacuum field amplitude, which results in the Purcell effect. The reduction of mode volume leads to an increase of the Purcell factor, as for the discussed range of diameters the mode volume decreases faster than the Q factors (see the inset of Fig. 1). For the decay of the signal over the first order of magnitude, the deviation from an exponential decay is rather weak. Straight lines have been added to fit a T_1 time

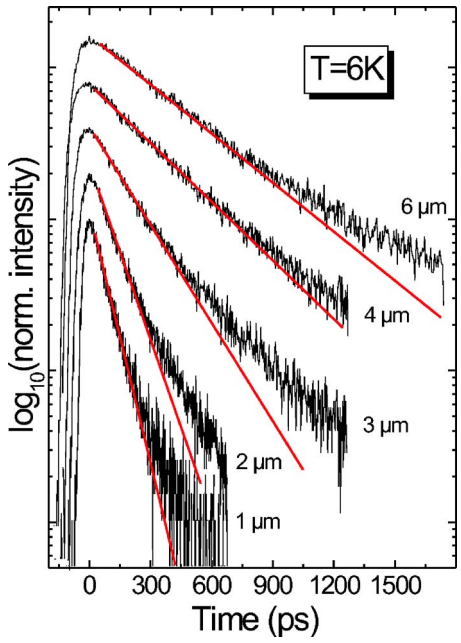

FIG. 2. (Color online) Low excitation time-resolved PL emission for micropillars with different diameters. The excitation power density was 1.3 kW cm^{-2}. The decay times corresponding to the single exponential fits shown by the solid lines are 400 ps (6 μm), 315 ps (4 μm), 200 ps (3 μm), 110 ps (2 μm), and 80 ps (1 μm). For clarity, the traces have been shifted vertically.

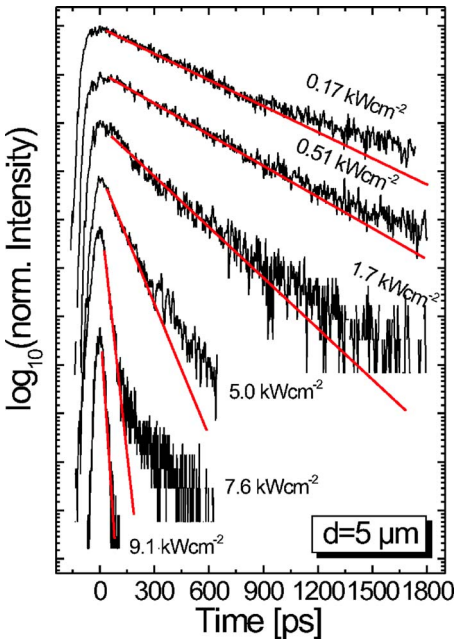

FIG. 3. (Color online) PL decay curves of a 5-μm cavity at different excitation powers. The decay times corresponding to the single exponential fits shown by the solid lines are 550 ps (0.17 kW cm^{-2}), 475 ps (0.51 kW cm^{-2}), 265 ps (1.7 kW cm^{-2}), 120 ps (5.0 kW cm^{-2}), 30 ps (7.6 kW cm^{-2}), and 20 ps (9.1 kW cm^{-2}). T=6 K. For clarity, the traces have been shifted vertically.

to the initial decay. However, on a larger scale the decay data clearly reveal a nonexponential character.

Here we note explicitly that the data cannot be described by biexponential or stretched exponential decay forms. While such forms naturally can match the data better than monoexponential decays, as they involve more fit parameters, they still result in considerable deviations from the data. Good agreement can generally only be reached by multiexponential decays involving a large number of parameters without physical meaning. Biexponential forms would be appropriate if there were two independent decay channels, each with a considerable contribution to the emission. Potential candidates for additional decay channels besides the excitonic one such as spin-dark excitons, charged excitons, and so on will be explicitly ruled out by the arguments given below.

To obtain more insight into the emission dynamics, we have varied the excitation power density P_{exc}. Figure 3 shows the time-resolved emission of a 5-μm pillar for different P_{exc} at an excitation wavelength of 800 nm. With increasing power, the decay becomes generally faster. Even for the lowest P_{exc}, for which we could record a time-resolved signal, no saturated, power-independent decay is found. For the highest excitation powers, rise and initial decay become more and more symmetric with respect to the signal maximum, indicating that the resonator has been pushed into the stimulated emission regime. Similar behaviors have been observed for pillars with other diameters.

First, we need to address the question, to what extent the observed dependencies regarding cavity size and excitation power are influenced by nonradiative decay channels, such as traps at the etched cavity sidewalls. Increasing importance of such traps with decreasing cavity diameter might also lead to the lifetime shortening observed in Fig. 2. To analyze this effect we have performed studies at varying temperatures. For $T>50$ K thermal emission out of the QD confinement becomes important, leading to a drop of PL intensity. At lower T, however, the integrated intensity is constant and also the decay times do not vary with temperature, which indicates a negligible influence of nonradiative decay. In this regime, the emitter linewidth $\Delta\lambda_e$ clearly falls below the cavity mode linewidth $\Delta\lambda_c$, which is a prerequirement for the observation of the Purcell effect.

The minor importance of nonradiative decay is also supported by a variation of the experiment, where the excitation wavelength is changed to 860 nm, which is slightly above the resonator stop-band edge, but below the GaAs barrier and into the wetting layer. This wavelength shift affects carrier capture and relaxation, but should not influence the cavity size dependence of the decay rate. However, it would be of importance if nonradiative decay were relevant, as for excitation above the barrier the photogenerated carriers may diffuse to the cavity sidewalls, while for excitation into the narrow wetting layer (which is subject to carrier localization effects at low temperatures) diffusion to the sidewalls is strongly hampered. Our data show no change in the decay rate shortening with decreasing cavity size for the two excitation conditions. The entirety of these tests allows us to relate the PL decay time to the radiative decay.

Different reasons for a deviation of the PL emission dynamics from an exponential decay need to be considered. For

very low excitation power, contributions from exciton complexes such as biexcitons can be ruled out. However, charged exciton complexes may be formed due to unintentional background doping, for example. We have tested the presence of residual charge carriers on a QD reference sample by Faraday rotation measurements[27] in a magnetic field normal to the heterostructure growth direction. Presence of free carriers would lead to observation of pronounced spin quantum beats which last longer than the exciton lifetime. As such beats could not be observed, we can safely conclude that the vast majority of QDs is undoped.

Further, in the present case the excitation was nonresonant, allowing for fast spin relaxation in the barriers. Therefore not only spin bright excitons are formed, but also spin dark excitons, which can recombine radiatively only after a spin flip. Previous investigations have shown that, at cryogenic temperatures, spin flips are strongly suppressed for carriers in the QD ground states. For electrons the only viable mechanism seems to be the hyperfine interaction with the lattice nuclei, while spin-orbit interaction has been shown to give spin-flip rates in the kHz range only, corresponding to much longer time scales than the ones considered here.[28] Spin-orbit interaction is also the only viable mechanism for the holes, but at low temperatures a two-phonon process is required to induce a spin flip.[29] In agreement with these considerations, exciton spin-flip times have been reported which are much longer than its radiative decay time.[30]

If feeding of the spin-bright exciton reservoir from the reservoir of dark excitons were important, two time scales would be relevant: Apart from the bright exciton decay during times <1 ns the dark exciton background would decay on time scales of nanoseconds or longer. From the study of a QD reference sample we find that no such background can be identified at cryogenic temperatures. For the time scales of interest it would appear as contribution to the constant background due to dark counts, which does not affect the decay analysis, as this background is subtracted. Thus, also the dark exciton states cannot be thought of as origin of the nonexponential decay at the used low temperatures. However, a strong background with decay times in the few ns range could be observed by raising the temperatures to a few tens of K, where the thermally induced phonon population can lead to flip processes through spin-orbit coupling. This is confirmed by the background decay time shortening strongly with increasing temperature.

IV. THEORETICAL MODEL

The aim of this section is to outline a theoretical model for the PL dynamics of QDs, which includes population effects in the carrier system, the many-body interaction between the carriers as well as their interaction with the quantized light field within a microcavity.

QDs are often compared to atomic systems due to the appearance of localized states with discrete energies. However, QDs usually contain many electronic states and excitations involve many electrons and holes, which are influenced by the Coulomb interaction. Additional carriers in the WL states contribute to screening and dephasing which—together with scattering processes among the localized carriers—weakens correlations between electrons and holes.

This situation differs fundamentally from light-matter interaction of atomic two-level systems, which are often used for a simplified analysis of QDs. A two-level model is applicable if the optical field couples resonantly only to two electronic levels *and* if the excitation involves only a single electron. In this case the appearance of an electron in the upper state is inescapably linked to the nonexistence of an electron in the lower state. In the semiconductor language, electron and hole populations are fully correlated. As a consequence, the time-resolved PL of two-level systems shows an exponential decay.

To describe the QD PL, we use the SLE for a system consisting of interacting charge carriers and a quantized light field, which has previously been applied to quantum wells.[17] The SLE describe the coupled dynamics of the electron- and hole-population $f_\alpha^{e,h}$, the generalized photon population $\langle \hat{b}_q^\dagger \hat{b}_{q'} \rangle$, and the photon-assisted polarization $\langle \hat{b}_q^\dagger \hat{h}_\alpha \hat{e}_\alpha \rangle$, in the incoherent regime:

$$i\hbar \frac{d}{dt} f_\alpha^{(e,h)}\Big|_{\text{opt}} = 2i \,\text{Re} \sum_q g_{q\alpha}^* \langle \hat{b}_q^\dagger \hat{h}_\alpha \hat{e}_\alpha \rangle, \tag{3}$$

$$i\hbar \frac{d}{dt} \langle \hat{b}_q^\dagger \hat{b}_{q'} \rangle = \hbar(\omega_{q'} - \omega_q^*) \langle \hat{b}_q^\dagger \hat{b}_{q'} \rangle - \sum_\alpha (g_{q'\alpha}^* \langle \hat{b}_q^\dagger \hat{h}_\alpha \hat{e}_\alpha \rangle - g_{q\alpha} \langle \hat{b}_{q'}^\dagger \hat{h}_\alpha \hat{e}_\alpha \rangle^*), \tag{4}$$

$$\begin{aligned} i\hbar \frac{d}{dt} \langle \hat{b}_q^\dagger \hat{h}_\alpha \hat{e}_\alpha \rangle &= (\tilde{\epsilon}_\alpha^e + \tilde{\epsilon}_\alpha^h - \hbar\omega_q^*) \langle \hat{b}_q^\dagger \hat{h}_\alpha \hat{e}_\alpha \rangle - (1 - f_\alpha^e - f_\alpha^h) \sum_\beta V_{\alpha\beta} \langle \hat{b}_q^\dagger \hat{h}_\beta \hat{e}_\beta \rangle \\ &\quad - (1 - f_\alpha^e - f_\alpha^h) \sum_{q'} g_{q'\alpha} \langle \hat{b}_q^\dagger \hat{b}_{q'} \rangle + g_{q\alpha} (f_\alpha^e f_\alpha^h + \Omega_{q,\alpha}^{cor}). \end{aligned} \tag{5}$$

Here, $\hat{e}_\alpha^\dagger$, $\hat{e}_\alpha$, and ϵ_α^e denote the creation and annihilation operators and the single-particle energy of an electron in state $\phi_\alpha^e(\vec{r})$. The corresponding quantities for the holes are $\hat{h}_\alpha^\dagger$, $\hat{h}_\alpha$, ϵ_α^h, and $\phi_\alpha^h(\vec{r})$. The states for charge carriers are either delocalized WL or localized QD states. The operator $\hat{b}_q^\dagger$ ($\hat{b}_q$) creates (destroys) a photon in the optical mode q, which is characterized by the complex resonance frequency ω_q and the transversal mode-pattern $\vec{u}_q(\vec{r})$. The light-matter coupling is determined by $g_{q\alpha} \propto \int d^3r \phi_\alpha^{e*}(\vec{r}) e\vec{r}\vec{u}_q(\vec{r}) \phi_\alpha^h(\vec{r})$. The exchange-Coulomb matrix elements are denoted by $V_{\alpha\beta}$ and the single-particle energies including Hartree-Fock renormalizations are given by $\tilde{\epsilon}_\alpha^{(e,h)}$. The population changes due to scattering are treated in a relaxation time approximation.

Equations (3) and (4) show that the dynamics of the carriers and photons are driven by the photon-assisted polarization, which is governed by Eq. (5). The first term on the right hand side of Eq. (5) describes the free evolution, while the second term is responsible for excitonic resonances in the spectrum. In the last line of Eq. (5), the first term describes stimulated emission or absorption. The other two terms con-

stitute the source due to spontaneous emission, which dominates over the stimulated emission term for weak excitations. Nevertheless, in high-Q microcavities, the reabsorption of photons can modify the results for the time-resolved emission even for weak excitation. On the Hartree-Fock level (corresponding to uncorrelated carriers) the source term is given by $g_{q\alpha}f_\alpha^e f_\alpha^h$. Correlations due to Coulomb interaction of carriers are included in $\Omega_{q,\alpha}^{cor}$ and are evaluated on singlet level.[31] We investigated the influence of higher-order contributions on doublet level. They are discussed in Ref. 32, and we find that they play no important role in the presence of the feedback provided by the cavity.

To gain additional insight into the physics described by the SLE, we use—only for the following discussion in this paragraph—some simplifications: We disregard stimulated emission and absorption and neglect the Coulomb interaction. The adiabatic solution of Eq. (5) then yields for the population dynamics

$$\frac{d}{dt} f_\alpha^{(e,h)}\big|_{\text{opt}} = -\frac{f_\alpha^e f_\alpha^h}{\tau_{\text{sp}}}, \tag{6}$$

where τ_{sp} is the time constant for spontaneous emission. The HF contribution to the source term $f_\alpha^e f_\alpha^h$ clearly leads to a nonexponential decay. Furthermore, the rate of decay depends on the carrier density and is higher for larger population. For the calculations presented below, none of the mentioned simplifications have been made: stimulated emission and absorption are included and Coulomb effects such as, corrections to the HF factorization of the source term of spontaneous emission are considered.

The discussed experiments can be used to distinguish between the two regimes of fully correlated electron-hole pairs, leading to an exponential decay of the PL, and partially correlated carriers with a nonexponential PL decay. As one is typically interested in the luminescence decay over a ns time scale rather than the initial excitation and relaxation of the system (which takes place on a ps time scale), we focus here on the dynamics that occurs after the system has been excited and the coherent polarization has decayed due to dephasing. In this incoherent regime we can use a Fermi-Dirac distribution of carriers in the WL and QD states and zero photons in the cavity as our initial conditions and evolve the system according to Eqs. (3)–(5).

In order to correctly account for the effects of the size distribution of the QDs (different transition energies), their spatial distribution inside the cavity, and the different dipole orientations (different coupling matrix elements), it is not sufficient to analyze the equations for a single dot with averaged properties. Instead it is necessary to solve the SLE for an entire ensemble of different QDs. For our calculation we take only a fraction of the total number of QDs with a transition frequency close to that of the relevant cavity modes. Therefore the effective density of QDs resonantly interacting with the cavity mode is assumed to be 3×10^9 cm^{-2}, distributed in an interval of approximately 1.5 meV.

The individual QDs are modeled with a harmonic confinement potential in the WL plane and a steplike confinement in growth direction. The strength of the harmonic confinement is varied for different QDs to account for the inhomogeneous broadening typically observed in this material system. We restrict our analysis to QDs with s and p shells for electrons and holes.

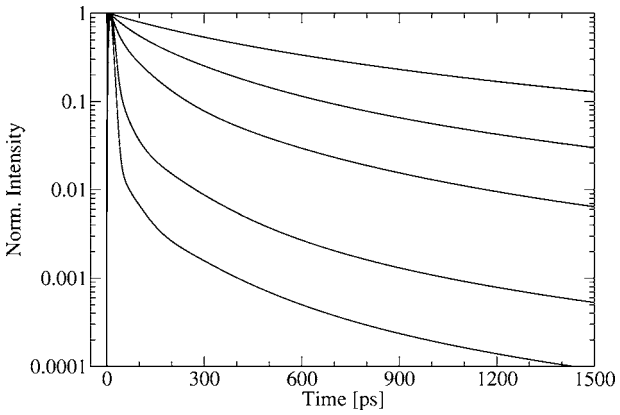

FIG. 4. Calculated PL for an ensemble of QDs in a 6-μm-diameter pillar microcavity with initial carrier densities from 1×10^9 cm^{-2} to 5×10^9 cm^{-2} in equidistant steps from top to bottom. For better comparison the results are normalized.

The transverse mode-pattern and resonance frequencies ω_q^{res} of the optical modes are calculated using a three-dimensional transfer-matrix approach (for details, see Ref. 26). The corresponding quality factors Q are obtained from the experiment. The complex resonance frequency is then given by $\omega_q=\omega_q^{\text{res}}(1-i/Q)$. While it is sufficient to include only one resonant mode for the smaller pillar, for the larger pillars several modes have to be taken into account. The coupling between different modes is neglected, $\langle\hat{b}_q^\dagger\hat{b}_{q'}\rangle\approx\delta_{qq'}\langle\hat{b}_q^\dagger\hat{b}_q\rangle$. Besides the resonant modes, which are characterized by their large Q values and pronounced peak structure in a transmission spectrum, there exists a background contribution from the continuum of leaky modes. In order to include their influence, we assume that the background contribution consists of a fraction of the continuum of modes of the homogeneous space. The size of this fraction can be estimated by counting the plane waves that (i) either reach the sidewalls of the micropillar in an angle smaller than the critical angle of total internal reflection, or (ii) have a momentum component $k_\parallel$ along the pillar axis that lies outside the stopband of the DBR and can therefore immediately escape from the cavity.

In Fig. 4 we show the number of photons in the fundamental mode leaving the cavity per unit time. Different initial carrier densities are used to model the variation of the excitation power in the experiment. The nonexponential decay of the signal is clearly evident. Furthermore, the rapidness of the decay strongly depends on the initial carrier density, which corresponds to different pump intensities in the experiment. This shows that it is not meaningful to introduce a decay time that depends only on the photonic density of states without including the influence of the carrier system. Instead, a thorough analysis of time-resolved PL signals has to take both the carrier system and the photonic system into account.

It should be noted that for strong optical fields the generated carrier density depends in a nonlinear manner on the

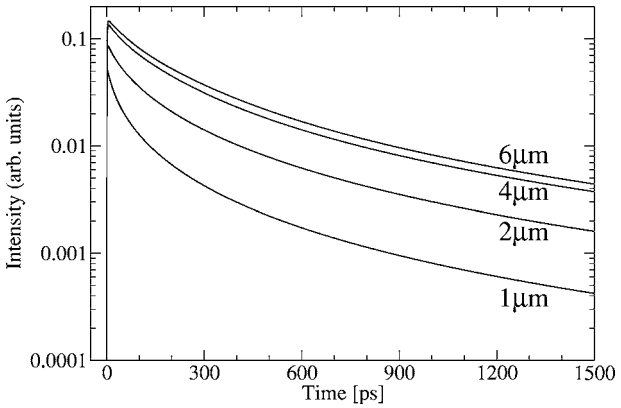

FIG. 5. Calculated PL of QDs in a pillar microcavities with various diameters for an initial carrier density of 2×10^9 cm^{-2}.

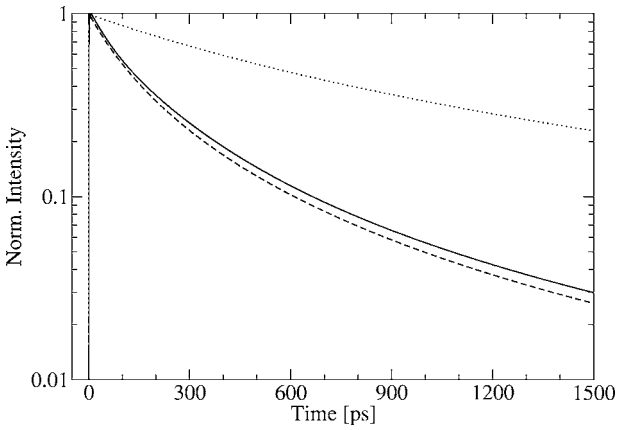

FIG. 6. Calculated PL of an ensemble of QDs with inhomogeneous broadening (solid line), for identical QDs with maximum coupling strength and on-resonance transitions (dashed line), and for identical QDs with averaged coupling strength (dotted). The pillar diameter is 6 μm and the initial carrier density is 2×10^9 cm^{-2}.

pulse intensity due to saturation effects. It is not the purpose of the paper to quantify these optical nonlinearities together with the subsequent carrier relaxation and to directly connect experimental pump intensities and the resulting carrier densities. Instead we focus on the physics of the recombination dynamics and emphasize the strong dependence of the time-resolved PL decay on the carrier density in the system.

The calculated PL for fixed initial carrier density but different diameters of the micropillar cavity is displayed in Fig. 5. The smaller pillars show a faster decay in connection with a larger Purcell factor, as has been discussed in Sec. III. The different heights of the curves can mainly be attributed to the fact that in larger pillars more carriers distributed over more QDs take part in the recombination dynamics.

Frequently it is argued that the nonexponential decay observed in PL measurements stems from a superposition of many exponential PL signals of various emitters with different cavity positions. The role of an inhomogeneous distribution of QDs is analyzed in Fig. 6. The solid line represents the calculated decay of the time-resolved PL from an ensemble of QDs with various cavity positions and fluctuations of the transition energies and dipole moments (same as in Figs. 4 and 5). For comparison, the dotted line shows the result for identical QDs with averaged values for mode strength, cavity field, transition energy, and dipole coupling. While the decay remains nonexponential, the decay rate is strongly underestimated. If identical QDs with maximum values for mode strength, cavity field, and dipole coupling as well as resonant transition energies are assumed (dashed line), the decay rate is slightly overestimated in the example with practically the same shape as for the inhomogeneous QD distribution. This result shows that the QDs with efficient coupling to the cavity field dominate the emission properties. The nonexponential character of the decay is only weakly determined by inhomogeneous distribution effects.

The deviations of the measured from the calculated results close to time $t=0$ and in particular the somewhat slower raise of the PL signal observed in the experiment can be attributed partially to the fact that the optical carrier generation was not modeled and that the experimental setup has only a finite time resolution. Note that we did not adjust the calculations to have a quantitative agreement between experiment and theory. Too many parameters, such as size and composition of the QDs, are unknown in detail.

V. SUMMARY

A microscopic description of the QD emission, based on the "semiconductor luminescence equations" including many-body Coulomb effects, shows the appearance of a nonexponential decay that is intimately connected with the intensity dependence of the decay from weak to strong excitation conditions. The results explain the time-resolved PL of QDs in pillar microcavities. Other origins such as contributions from spin-dark excitons, charged excitons, etc., have been ruled out as dominant contributions to the observations for the presented experiments.

ACKNOWLEDGMENTS

This work was supported by the research group "Quantum Optics in Semiconductor Nanostructures" funded by the Deutsche Forschungsgemeinschaft. The Bremen Group acknowledges a grant for CPU time at the Forschungszentrum Jülich, Germany.

[1] E. M. Purcell, Phys. Rev. **69**, 681 (1946).
[2] B. Gayral, J. M. Gérard, A. Lemaitre, C. Dupuis, L. Manin, and J. L. Pelouard, Appl. Phys. Lett. **75**, 1908 (1999).
[3] J. M. Gérard, B. Sermage, B. Gayral, B. Legrand, E. Costard, and V. Thierry-Mieg, Phys. Rev. Lett. **81**, 1110 (1998).
[4] L. A. Graham, D. L. Huffaker, and D. G. Deppe, Appl. Phys. Lett. **74**, 2408 (1999).
[5] M. Bayer, F. Weidner, A. Larionov, A. McDonald, A. Forchel,

and T. L. Reinecke, Phys. Rev. Lett. **86**, 3168 (2001); B. Ohnesorge, M. Bayer, A. Forchel, J. P. Reithmeier, N. A. Gippius, and S. G. Tikhodeev, Phys. Rev. B **56**, R4367 (1997).

[6] G. S. Solomon, M. Pelton, and Y. Yamamoto, Phys. Rev. Lett. **86**, 3903 (2001).

[7] C. J. M. Smith, H. Benisty, D. Labilloy, U. Oesterle, R. Houdr, T. F. Krauss, R. M. De La Rue, and C. Weisbuch, Electron. Lett. **35**, 228 (1999).

[8] P. Meystre and M. Sargent, *Elements of Quantum Optics* (Springer, Berlin, 1999).

[9] P. Lodahl, A. F. van Driel, I. S. Nikolaev, A. Irman, K. Overgaag, D. Vanmaekelbergh, and W. L. Vos, Nature (London) **430**, 654 (2004).

[10] Xudong Fan, Mark C. Lonergan, Yuzhong Zhang, and Hailin Wang, Phys. Rev. B **64**, 115310 (2001).

[11] W. Fang, J. Y. Xu, A. Yamilov, H. Cao, Y. Ma, S. T. Ho, and G. S. Solomon, Opt. Lett. **27**, 948 (2002).

[12] I. L. Krestnikov, N. N. Ledentsov, A. Hoffmann, D. Bimberg, A. V. Sakharov, W. V. Lundin, A. F. Tsatsulnikov, A. S. Usikov, Z. I. Alferov, Y. G. Musikhin, and D. Gerthsern, Phys. Rev. B **66**, 155310 (2002).

[13] R. A. Oliver, G. A. D. Briggs, M. J. Kappers, C. J. Humphreys, S. Yasin, J. H. Rice, J. D. Smith, and R. A. Taylor, Appl. Phys. Lett. **83**, 755 (2003).

[14] T. Auer, T. Berstermann, M. Bayer, V. Stavarache, D. Reuter, and A. Wieck, Phys. Rev. B (to be published).

[15] See, for example, M. Bayer, G. Ortner, O. Stern, A. Kuther, A. A. Gorbunov, A. Forchel, P. Hawrylak, S. Fafard, K. Hinzer, T. L. Reinecke, S. N. Walck, J. P. Reithmaier, F. Klopf, and F. Schäfer, Phys. Rev. B **65**, 195315 (2002).

[16] See, for example, B. Patton, W. Langbein, and U. Woggon, Phys. Rev. B **68**, 125316 (2003).

[17] M. Kira, F. Jahnke, and S. W. Koch, Phys. Rev. Lett. **81**, 3263 (1998).

[18] Details of the fabrication process are found in M. Röhner, J. P. Reithmaier, A. Forchel, F. Schäfer, and H. Zull, Appl. Phys. Lett. **71**, 488 (1997).

[19] J. P. Reithmaier, G. Sek, A. Löffler, C. Hofmann, S. Kuhn, S. Reitzenstein, L. V. Keldysh, V. D. Kulakovskii, T. L. Reinecke, and A. Forchel, Nature (London) **432**, 197 (2004).

[20] J. M. Gérard, D. Barrier, J. Y. Marzin, R. Kuszelewicz, L. Manin, E. Costard, V. Thierry-Mieg, and T. Rivera, Appl. Phys. Lett. **69**, 449 (1996).

[21] J. P. Reithmaier, M. Röhner, H. Zull, F. Schäfer, A. Forchel, P. A. Knipp, and T. L. Reinecke, Phys. Rev. Lett. **78**, 378 (1997).

[22] T. Gutbrod, M. Bayer, A. Forchel, J. P. Reithmaier, T. L. Reinecke, S. Rudin, and P. A. Knipp, Phys. Rev. B **57**, 9950 (1998); T. Gutbrod, M. Bayer, A. Forchel, P. A. Knipp, T. L. Reinecke, A. Tartakovskii, V. D. Kulakovskii, N. A. Gippius, and S. G. Tikhodeev, *ibid.* **59**, 2223 (1999).

[23] M. Pelton, C. Santori, J. Vuckovic, B. Zhang, G. S. Solomon, J. Plant, and Y. Yamamoto, Phys. Rev. Lett. **89**, 233602 (2002).

[24] A. Löffler, J. P. Reithmaier, G. Sek, C. Hofmann, S. Reitzenstein, M. Kamp, and A. Forchel, Appl. Phys. Lett. **86**, 111105 (2005).

[25] A. Daraei, A. Tahraoui, D. Sanvitto, J. A. Timpson, P. W. Fry, M. Hopkinson, P. S. S. Guimaraes, H. Vinck, D. M. Whittaker, M. S. Skolnick, and A. M. Fox, Appl. Phys. Lett. **86**, 051113 (2006).

[26] M. Benyoucef, S. M. Ulrich, P. Michler, J. Wiersig, F. Jahnke, and A. Forchel, New J. Phys. **6**, 91 (2004).

[27] See, for example, *Semiconductor Spintronics and Quantum Computation*, edited by D. D. Awschalom, D. Loss, and N. Samarth (Springer-Verlag, Heidelberg, 2002).

[28] T. Brandes and T. Vorrath, Phys. Rev. B **66**, 075341 (2002); G. L. J. A. Rikken and P. Wyder, Phys. Rev. Lett. **94**, 016601 (2005); R. Hanson, B. Witkamp, L. M. K. Vandersypen, L. H. Willems van Beveren, J. M. Elzerman, and L. P. Kouwenhoven, *ibid.* **91**, 196802 (2003).

[29] A. V. Khaetskii, D. Loss, and L. Glazman, Phys. Rev. Lett. **88**, 186802 (2002); I. A. Merkulov, Al. L. Efros, and M. Rosen, Phys. Rev. B **65**, 205309 (2002); R. de Sousa and S. Das Sarma, *ibid.* **67**, 033301 (2003); L. M. Woods, T. L. Reinecke, and Y. Lyanda-Geller, *ibid.* **66**, 161318 (2002); L. M. Woods, T. L. Reinecke, and R. Kotlyar, *ibid.* **69**, 125330 (2004).

[30] M. Paillard, X. Marie, P. Renucci, T. Amand, A. Jbeli, and J. M. Gérard, Phys. Rev. Lett. **86**, 1634 (2001).

[31] F. Jahnke, M. Kira, W. Hoyer, and S. W. Koch, Phys. Status Solidi B **221**, 189 (2000).

[32] N. Baer, C. Gias, J. Wiersig, and F. Jahnke, Eur. Phys. J. B **40**, 411 (2006).